ISSN 0967-0912, Steel in Translation, 2009, Vol. 39, No. 2, pp. 146–151. © Allerton Press, Inc., 2009.
Original Russian Text © Yu.A. Samoilovich, 2009, published in "Stal'," 2009, No. 2, pp. 20–25.

Destruction of the Dendritic Bridge in Soft Reduction of Continuous-Cast Slab

Yu. A. Samoilovich
OAO VNIIMT, Yekaterinburg, Russia

DOI: 10.3103/S0967091209020132

In order to improve the properties of structural steels, the crystalline structure and chemical composition of the continuous-cast billet must be more isotropic. A promising approach is soft reduction of the billet by a special (dynamic) section in the roller track of the continuous-casting machine [1–6]. We now consider some examples of soft reduction.

Industrial tests of soft reduction in the continuous casting of steel slabs on a vertical machine at OAO Severstal were described in [1, 2]. The extent of the columnar-crystal zone was halved (from 80 to 40 mm) by 2–4% reduction, at a casting rate of 0.55 m/min, according to [1].

Soft reduction increased the proportion of melts with an axial chemical-inhomogeneity score no greater than 1 from 68.9 to 95.8%, according to [2].

At the International Conference on Continuous Steel Casting (Madrid, 1987), the use of soft reduction in continuous casting of round and square bar billet was reported [3, 4]. Soft reduction of continuous-cast bearing-steel billet (diameter 350 mm) significantly reduced the axial inhomogeneity of carbon, according to [3]: the excess carbon content in the axial zone of the billet was 0.05–0.07% after soft reduction (~1.6% of the billet diameter) but 0.25–0.35% C without reduction. The continuous casting of corrosion-resistant steel in 265 × 265 mm blooms on a curvilinear machine was considered in [4]. The reduction was produced by three pairs of rollers at distances of 17.7, 19.8, and 22 m from the melt meniscus in the mold. The casting rate was 0.81–0.89 m/min; the total reduction was 4–7 mm.

Soft reduction reduced the axial porosity of the cast billet by a factor of around 1.5–3, according to [4].

Two main factors are responsible for the axial chemical inhomogeneity in continuous-cast slabs, according to [7]:

1) the formation of bridges (crosslinks) in the nonsolidifying part of the billet, preventing melt access to the shrinkage cavities in the center of the billet;

2) swelling of the shell of the solidifying billet due to the ferrostatic pressure of the melt in the nonsolidifying part, with a sufficiently large distance between the supporting rollers.

We now consider the theoretical principles underlying the reduction in axial chemical inhomogeneity of continuous-cast slabs by soft reduction, taking account of both the factors noted in [7].

We begin with the assumption that the reduced axial inhomogeneity in the billet is due to destruction of the dendritic bridges that are formed by the growing crystals (columnar or equiaxial crystals) and hinder the melt's access to the shrinkage zones in the central part of the solidifying billets. This is not an original suggestion. Under the influence of soft reduction, "the core is strengthened, the liquational material is driven out, and the dendrites are broken down, with improvement in axial structure of the ingot," according to [6]. We note that the dendrite fracture is consistent with the shrinkage of the columnar-crystal zone relative to the equiaxial-crystal zone, noted in [1].

In the present work, we attempt quantitative estimation of the probability that the bridges preventing melt access to the shrinkage cavities (pores) in the axial zone of the billet will disintegrate under the action of soft reduction.

In production tests, it is found that soft reduction is most effective when the liquid-phase content S within the two-phase zone of the solidifying billet is 20–80%. When the content of solid phase $\Psi = 1 - S$ is below the lower limit $\Psi_1 = 0.2$, the solidifying metal in the two-phase zone consists of a suspension of crystals in melt, and the application of external forces leads to motion of the suspension as a whole within the liquid core (the nonsolidifying part of the billet), without significant improvement in the cast structure.

On reaching the critical quantity of solid phase $\Psi_{cr} = 0.2$, the crystals suspended in the melt, together with the oriented (columnar) dendrites, form a dendritic skeleton (filled with melt) capable of resisting the applied external force.

The application of compressive force to the shell of the cast billet by the supporting rollers may fracture the dendritic skeleton; this does not always improve the cast structure. Evidently, when the solid-phase content in the two-phase zone exceeds the upper limit $\Psi_2 = 0.8$, the resistance of the dendritic skeleton to the external force sharply rises, and soft reduction may increase the number of internal cracks in the solidifying billet or damage the rollers. Obviously, the behavior of the dendritic skeleton under the action of external compressive forces depends significantly on the mechanical properties of the steel close to the solidus temperature of the steel and also on the structure of the dendritic skeleton and the geometric parameters of the section of billet subjected to soft reduction. Because the corresponding continuum-mechanics problem is complex, there has been little study of soft reduction, which hinders its introduction in the continuous casting of various billets.

The physicomathematical formulation of the problem consists of two parts.

The first part includes the system of heat- and mass-transfer equations of the solidifying continuous-cast billet, whose solution determines the temperature field, the impurity concentration, and the quantity of solid phase within the billet's two-phase zone. This problem is solved on the basis of quasi-equilibrium models of the solidifying binary alloy, using numerical methods and computer technology [8–10]. The results of solution will not be discussed in the present work. Solution of the given system of equations permits the determination of the zone along the technological axis of the continuous-casting machine where $\Psi_1 \le \Psi \le \Psi_2$. Thus, the solution of these equations refines the location of the specialized roller section for soft reduction.

The second part of the problem includes equations whose solution must assist the researcher in specifying the soft-reduction parameters, taking account of the specifics of the process (the characteristics of the dendritic skeleton, the mechanical properties of the steel at high temperature, and the geometric parameters of the section of billet subject to soft reduction).

We now consider the simplest formulation of the continuum-mechanics problem of determining the stress–strain field of the dendritic bridge under the action of the compressive forces applied to the shell of the continuous-cast billet. The formulation of the problem employs some characteristics of the dendritic skeleton noted in [11, 12]. According to Bochvar, the solid–liquid state of the alloy is characterized by the formation of a relatively rigid skeleton of dendritic crystallites, with two characteristics: negligible plasticity and very low strength. Flexure tests of samples in the solid–liquid state show that, in fact, the alloy above the solidus temperature has a distinct and very low strength and negligible plasticity. Therefore, slight shrinkage stress exceeding the low strength will result in cracking. When the alloy completely solidifies, its plasticity rises sharply. With further slowing of shrinkage, even larger stress appears, and the strength remains low. No new cracks appear below the solidus, since hindered shrinkage is compensated by the high plasticity of the completely solid alloy [12].

Bochvar's picture of a dendritic skeleton characterized by high rigidity and negligible plasticity is confirmed by experimental data for the elastic modulus of carbon steel at high temperature (96% of the alloy's solidus temperature) [13].

These experiments, conducted by a dynamic method in the frequency range 0.1–15 Hz, lead to the unexpected conclusion that the elastic modulus of carbon steel in the range $T = (0.65–0.96)T_{sol}$ remains practically constant: $(0.9–1.2) \times 10^5$ MPa.

This result was confirmed in [14]; in those experiments, the elastic modulus of steel at 1200°C was 9×10^4 MPa. These results are fundamentally inconsistent with the widespread opinion that the elastic modulus of the steel declines monotonically with increase in temperature from 700 to 1300–1500°C, reaching 900–2000 MPa at 1400–1425°C [5, 15].

Evidently, this difference in the elastic modulus of steel at high temperature is due to the monotonic decrease in elastic modulus in the range 700–1450°C in static tests with prolonged holding of the samples at the control temperatures. With soft reduction of billet in a dynamic roller system, the external mechanical action on local sections of the two-phase zone is brief (seconds), and it is better to use the elastic modulus of steel obtained by the dynamic method.

After these preliminary remarks, we now present the mathematical formulation of the problem of determining the stresses and strains in the solid phase for several configurations of the dendritic skeleton. The traditional nonlinear-elasticity equations (disregarding plastic deformation) are used here, in the plane-deformation approximation [16]:

the equilibrium equations

$$\frac{\partial\sigma_x}{\partial x} + \frac{\partial\tau_{xy}}{\partial y} = 0, \quad \frac{\partial\tau_{xy}}{\partial x} + \frac{\partial\sigma_y}{\partial y} = 0, \quad \frac{\partial\sigma_z}{\partial z} = 0; \quad (1)$$

the equations describing the behavior of the solid phase

$$\begin{bmatrix}\sigma_x \\ \sigma_y \\ \tau_{xy}\end{bmatrix} = D\begin{bmatrix}\varepsilon_x \\ \varepsilon_y \\ \gamma_{xy}\end{bmatrix}; \quad (2)$$

the elastic-constant tensor of the ingot

$$D = \frac{E}{(1+\nu)(1-2\nu)}\begin{bmatrix}1-\nu & \nu & 0 \\ \nu & 1-\nu & 0 \\ 0 & 0 & \frac{1-2\nu}{2}\end{bmatrix}, \quad (3)$$

where the components of the stress tensor (σ_x, σ_y, τ_{xy}) and strain tensor (ε_x, ε_y, γ_{xy}) are shown; E is the elastic modulus; ν is Poisson's ratio. The external pressures P_c, P_f applied to the boundaries of the given section of billet take the form

$$P_c = F/(L_1 L_{co}), \quad P_f = \rho g H, \quad (4)$$

where F is the compressive force applied to the rollers of the dynamic section; H is the height of the liquid-phase column; L_1 is the roller length; L_{co} is the length of the generatrix of the roller's contact zone with the billet surface: $L_{co} = 0.035R\arccos(1 - d/R)$, where R is the roller radius; d is the degree of billet reduction between a single pair of rollers. To Eqs. (1)–(3), we need to add equations taking into account that soft reduction acts on a heterogenous melt–crystal system, so that the dendritic skeleton of the solidifying billet is subjected to the mechanical action of the liquid phase in the space between the dendritic branches. The hydrodynamic pressure in the melt between the dendrites may be determined from the equation

$$\frac{\rho g m}{A}\frac{\partial P}{\partial t} = \operatorname{div}(k\operatorname{grad}P), \tag{5}$$

obtained from the continuity equations of the heterogeneous melt–crystal system using the following notation [17]: ρ is the density; k is the filtration coefficient of the melt in the dendrite network; m is the proportion of liquid phase (melt) in the heterogeneous system (the cross section of the two-phase zone in the terminology of [10]); A is the bulk-compression modulus of the melt; $g = 9.81$ m/s^2.

The compressive pressure P_c is calculated with specification of the forces F applied to the rollers and the contact area S between the roller and billet: $P_c = F/S$. In subsequent calculations, we assume that the force F in the vicinity of a single pair of rollers varies according to the formula

$$F = F_0\{1 - \exp[-B(t/t_1)^2]\}, \tag{6}$$

where F_0 is the limiting force; t is the time; B and t_1 are empirical constants. The parameters F_0, B, and t_1 are used in setting up the drive of the hydraulic cylinders that control the reduction in the dynamic roller section.

Before solving Eqs. (1)–(5), we determine the characteristics of the two-phase zone of the solidifying billet, taking account of the conditions of billet cooling, so as to identify the section of the continuous-casting line where soft reduction must be employed.

Consider a 315 × 2000 mm continuous cast 10Г2С steel slab. In this case, the recommended soft-reduction parameters are as follows [5]: beginning of the reduction zone at 25 m; end of the zone at 29.17 m; length of the reduction zone 4.17 m; 12 roller pairs in the reduction zone; roller spacing 350 mm; roller radius 150 mm; casting rate 0.9 m/min; reduction per pair of rollers 0.5 mm; total reduction 6 mm.

Calculations of the solidification and cooling of slab billet (thickness 300 mm) were presented in [5]. The roller module applying soft reduction to the steel slab (at a casting rate of 0.9 m/min) must be 20–25 m from the melt meniscus in the mold. The ferrostatic pressure acting on the control element of the solidifying alloy (in the soft reduction zone) is calculated from the formula $P_f = \rho g H$. If $\rho = 6900$ kg/m^3, $g = 9.807$ m/s^2, and $h = 20$ m, we find that $P_f = \rho g H = 6900 \times 9.807 \times 20 = 1.353 \times 10^6$ kg/(m s^2) = 1.353 MPa, since 1 kg/(m s^2) = 1 Pa. Note that, for unexplained reasons, the value $P_f = 0.24$ MPa was used when $H = 25$ m in [5, p. 259].

The total reduction of the blank (6 mm) is applied by 12 roller pairs, with 0.5-mm reduction in each, according to [5].

Equations (1)–(6) are solved numerically by the finite-element method, with specification of the following properties of the steel close to the solidus temperature of carbon steel: $\rho = 7200$ kg/m^3; proportion of liquid phase (cross section) $m = 0.5$; bulk-compression modulus of melt $A = 1.738 \times 10^5$ MPa; elastic modulus of solid phase at the solidus temperature $E = 9 \times 10^4$ MPa [13, 14]; Poisson's ratio $\nu = 0.43$ [18]. In determining the filtration coefficient of liquid steel in the dendrite network, its dependence on the melt viscosity and structure of the porous medium is employed, on the basis of [17].

In the calculations, we assume that $F_0 = 100$–500 kN. Note that, on the basis of formulas for rolling and the introduction of a stamp in the metal, higher values of F_0 were calculated in [5].

In solving Eqs. (1)–(6), the configuration of the dendritic skeleton must be specified; this poses certain difficulties. We know from metallographic data for cast steel that, in general, the cross section of a continuous-cast billet may be divided into three zones: a solid crust at the surface of the billet, consisting of finely disperse crystallites; a zone of columnar structure; and a zone of equiaxial structure. The extent of the columnar zone is usually no more than 4–8 cm [1]; the equiaxial zone is filled with solid fragments (ranging from 0.5 to 2–3 mm) with no particular orientation. As yet, the data on dendrite growth in cooled-steel melt are insufficient for the prediction of the billet structure. Accordingly, in solving Eqs. (1)–(6), some of the most likely configurations of the dendritic bridge will be considered, so as to establish the stress state of the dendritic skeleton and the probability of bridge failure in specifying the external compressive forces in the soft-reduction zone.

The simplest configuration of the dendritic bridge, formed by direct junction of columnar dendrites growing from opposite sides of the billet, is shown in Fig. 1 (configuration 1).

When using the finite-element method, the area of the calculated section of the billet is represented as a grid containing ×2000 triangular elements, so as to ensure accurate solution. In the calculations, the distribution of the primary stress-tensor components (σ_x, σ_y, τ_{xy}) and the Mises numbers (stress intensities) within the solid crust of the billet and in solid fragments is determined. The distributions of the normal stress-tensor components (σ_x, σ_y) along the line AB (Fig. 1) are shown in Fig. 2 for the upper columnar dendrite, when

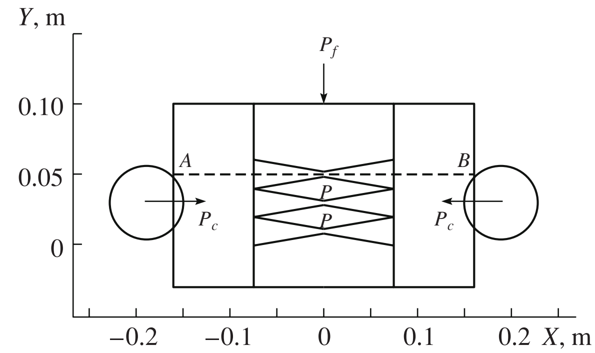

Fig. 1. Configuration of dendritic bridge in the central part of a continuous-cast billet in soft reduction (configuration 1).

$F_0 = 200$ kN, $B = 5$, and $t_1 = 0.5$ s. In addition, the stress intensity

$$\text{Mises} = \frac{1}{\sqrt{2}}\sqrt{(\sigma_x - \sigma_y)^2 + \sigma_y^2 + \sigma_x^2 + 6\tau_{xy}^2}, \quad (7)$$

corresponding to the plane-deformation model adopted in the calculations for the spatial coordinates X, Y is shown in Fig. 2.

It follows from Fig. 2 that the primary components of the stress tensor are negative (compressive) in the region adjacent to the solid crust of the solidifying billet (when $|X| \geq 7.5$ cm); in the central zone of the blank, they become positive, which corresponds to hazardous tensile stress. The maximum tensile stress and Mises function will appear in the junction section of columnar dendrites, in the median plane of the billet.

The dendritic bridge formed by the growth of three dendrites, two of which grow from left to right (A, B), while one (C) grows from right to left, is shown in Fig. 3 (configuration 2). The distribution of the primary stress-tensor components for bridge configuration 2 (Fig. 3) is radically different from that for the simplified configuration 1 (Fig. 1). In configuration 2, negative values of the normal components σ_x and σ_y and the Mises numbers predominate near the junction of the columnar dendrites. The tensile (positive) tangential stress is more dangerous; local maxima appear in the contact sections of the dendritic branches with one another and with the dense crust of the cast billet.

In Fig. 3, the circles denote sections of growing dendrites where shear strain of the metal predominates and the positive (tensile) tangential stress is a maximum.

The variation in tangential stress in sections *1*, *2*, and *3* (indicated by arrows in Fig. 3) over time is shown in Fig. 4. (For section *4*, the calculated tangential stress is practically the same as for section *3*.)

The configuration of the bridge formed from small (1–2 mm) solid fragments characteristic of the equiaxial-dendrite zone in continuous-cast steel billet is shown in Fig. 5 (configuration 3).

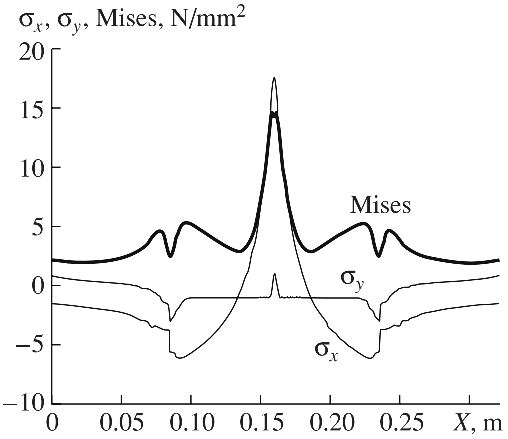

Fig. 2. Distribution of the stress-tensor components and Mises number along the line AB in configuration 1 with $F_0 = 200$ kN.

In this case, tensile tangential stress arises at the contact sections of individual dendritic blocks. The maximum tangential stress is observed at the junction of the upper level of the blocks with the left solid crust (see point Def in Fig. 5). This corresponds to the additional action of the melt's ferrostatic pressure at the upper level of the dendritic blocks. The variation in tangential stress at point Def is shown in Fig. 6 when $B = 5$ and $t_1 = 0.5$ s, for several values of F_0 in the range 100–500 kN. We see that the maximum tangential stress, established at $t \geq 1$ s, varies from 1.4 ($F_0 = 100$ kN) to 7 N/mm^2 ($F_0 = 500$ kN).

Given that the strength of carbon steel at the solidus temperature is 1–2 N/mm^2 [19, 20], we may assume that destruction of the dendritic bridge in Fig. 5 (configuration 3) is unavoidable at $F_0 \geq 200$–300 kN.

The distribution of the stresses σ_x, τ_{xy} and Mises numbers along the line AB intersecting the upper level of the bridge blocks (Fig. 5) is shown in Fig. 7, when $F_0 = 500$ kN and $t_1 = 1$ s. The curves in Fig. 7 confirm

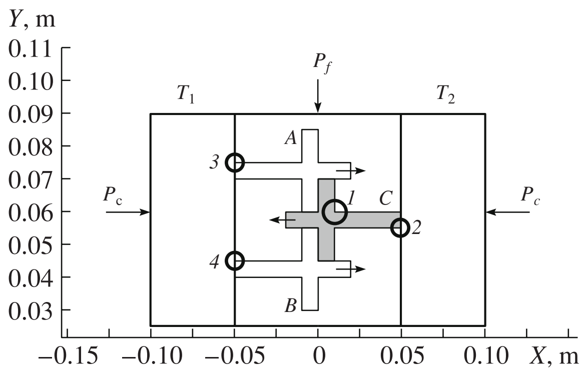

Fig. 3. Configuration of the bridge formed from three opposing dendrites (configuration 2): arrows *1*–*4* indicate sections where tensile tangential stress appears.

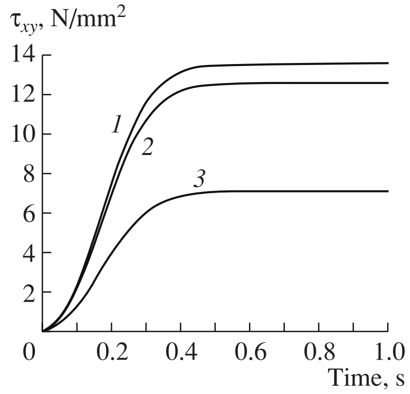

Fig. 4. Variation in tangential stress within sections *1–3* indicated by arrows in Fig. 3; explanation in text.

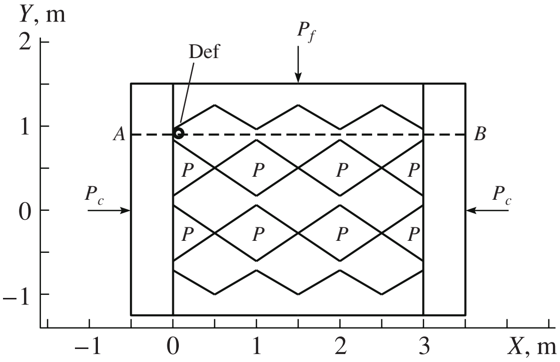

Fig. 5. Configuration of the bridge formed by a system of equiaxial crystallites in the central part of a continuous-cast billet (configuration 3): Def denotes the section of maximum tangential stress.

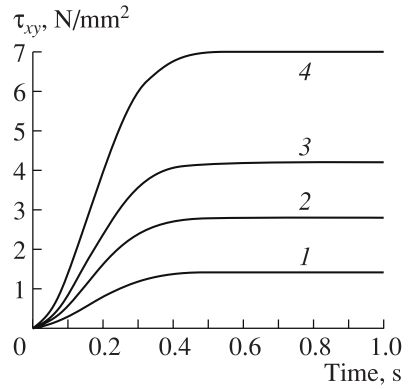

Fig. 6. Variation in tangential stress at point Def (Fig. 5), when the forces applied to the rollers in the soft reduction zone are 100 (*1*), 200 (*2*), 300 (*3*), and 500 (*4*) kN.

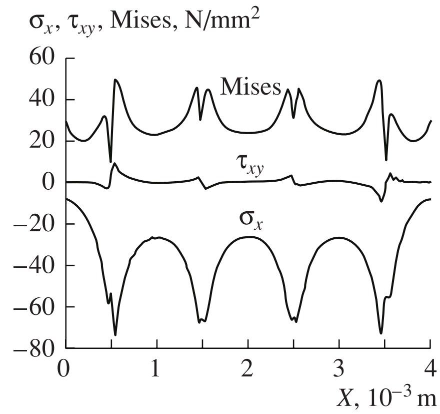

Fig. 7. Distribution of the normal and tangential stresses and the Mises number along the line *AB* in the cross section of the given section (Fig. 5).

the predominance of positive (tensile) tangential stress at the contact sections of individual solid fragments for the rigid skeleton formed by the intergrowth of small equiaxial dendrites. Note, in passing, the negative normal component (compression) of the stress tensor σ_x and the extremely large Mises number (stress intensity) in the contact sections of the blocks. This permits recommendations regarding the selection of failure conditions for the rigid dendritic skeleton with the bridge configurations in Figs. 3 and 5.

In strength theory, the failure probability of stressed parts is estimated on the basis of the following postulates:

failure is most likely under the action of tensile stress ($\sigma_x > 0$, $\sigma_y > 0$, $\tau_{xy} > 0$ in the present case);

the condition for probable failure of the crystallites is the energy relation

$$\text{Mises} \geq k\sigma_s, \quad (8)$$

where k is the strength margin; σ_s is the yield point of the steel in linear extension.

Both postulates may be used in estimating the failure probability of bridges in configuration 1 (Fig. 1). For the more realistic configurations in Figs. 3 and 5, however, the components of the stress tensor σ_x, σ_y are compressive, and failure is most likely under the action of tangential stress in the contact sections between individual branches of the dendrites.

Since the value of the Mises function is largely determined by the normal components of the stress tensor (σ_x, σ_y), it is better to use the failure condition

$$(\tau_{xy})_{\max} \geq k\sigma_s \quad (9)$$

for the bridge configurations in Figs. 3 and 5 (configurations 2 and 3).

Calculations permit the conclusion that, when bridges are formed by the intergrowth of dendritic branches, the tensile stress that arises at the contact sections of the dendritic branches under the action of soft reduction on a solidifying billet significantly exceeds the strength of the steel close to the solidus temperature. We may suppose that the improvement in billet quality under the action of soft reduction is due to bridge fracture, which improves the filtrational flow into the shrinkage pores in the central part of the billet and reduces the axial chemical inhomogeneity of the cast steel.

Given the stress state of the rigid dendritic skeleton in soft reduction, we recommend that the failure probability be estimated on the basis of the attainment of critical tangential stress in the contact sections of the dendritic branches, rather than on the basis of the Mises energy conditions.

REFERENCES

1. Lamukhin, A.M., Ziborov, A.V., Imgrunt, V.Ya., et al., Tests of the Soft Reduction System for a Continuous-Cast Slab with a Liquid Core, *Stal*, 2002, no. 3, pp. 57–59.
2. Stepanov, A.A., Ziborov, A.V., Kuntsov, N.I., et al., Producing Thick Sheet on a Vertical Roller-Conveyer System with Soft Reduction of the Continuous-Cast Billet, *Metallurg*, 2005, no. 6, p. 42.
3. Hayakama, S., Shinkai, M., and Kashima, T., Improvement of Center Quality of Continuous Cast Round Bloom with Soft Reduction, *Third European Conference on Continuous Casting*, Madrid, Spain, 1998, no. 1, pp. 225–233.
4. Sivesson, P., Wass, S., and Rodberg, B., Improvement of Center Porosity in Continuous-Casting Blooms by Mechanical Soft Reduction at the End of the Solidification Process, *Third European Conference on Continuous Casting*, Madrid, Spain, 1998, no. 1, pp. 213–225.
5. Budanov, L.V., Korzukhin, L.G., Parfenov, E.P., et al., *Mashiny nepreryvnogo lit'ya (teoriya i raschet)* (Continuous-Casting Machine: Theory and Calculation), Yekaterinburg: Marat, 2004.
6. Parshin, V.M. and Chertov, A.D., Quality Control of Continuous-Cast Billet, *Stal,* 2005, no. 1, pp. 20–29.
7. Kuklev, A.V., Sosini, V.V., and Pozdnyakov, V.A., Formation of Axial Chemical Inhomogeneity in Continuous-Cast Slabs, *Stal*, 2003, no. 8, pp. 71–75.
8. Samoilovich, Yu.A., *Formirovanie slitka* (Ingot Formation), Moscow: Metallurgiya, 1977.
9. *Teplovye protsessy pri nepreryvnom lit'e stali* (Thermal Processes in the Continuous Casting of Steel), Samoilovich, Yu.A., Ed., Moscow: Metallurgiya, 1982.
10. Borisov, V.T., *Teoriya dvukhfaznyoi zony metallicheskikh slitkov* (Theory of the Two-Phase Zone in Metal Ingots), Moscow: Metallurgiya, 1987.
11. Bochvar, A.A. and Zhadieva, O.S., Theory of Shrinkage in Alloys, *Tr. MITsMiZ* (Proceedings of Moscow Institute of Nonferrous Metals and Billet), Moscow: MITsMiZ, 1940, issue 9, pp. 534–545.
12. Bochvar, A.A. and Novikov, I.I., Solid–Liquid State of Alloys during Solidification, *Tekhnologiya tsvetnykh metallov* (Technology of Nonferrous Metals), Moscow: MITsMiZ, 1952, issue 23, pp. 5–23.
13. Udovik, O.A., Yakovkin, V.N., and Yakobshe, R.Ya., Elastic Characteristics of Low- and Moderate-Carbon Steel in the Range 20–1400°C, *Progressivnye sposoby polucheniya stal'nykh slitkov* (Progressive Methods of Steel-Ingot Production), Kiev: Institute Problem Lit'ya, 1980, pp. 121–127.
14. Thomas, B.G., Issues in Thermal-Mechanical Modeling of Casting Processes, *ISIJ Intern.,* 1995, vol. 35, no. 6, pp. 737–743.
15. Puhringer, O.M., Billet Formation in a Continuous-Casting Machine, *Ferrous Metals (Germany)*, 1976, no. 6, pp. 3–9.
16. Sedov, L.I., *Mekhanika sploshnoi sredy* (Continuum Mechanics), Moscow: Nauka, 1973, 2nd ed.
17. Samoilovich, Yu.A., *Kristallizatsiya slitka v elektromagnitnom pole* (Ingot Solidification in an Electromagnetic Field), Moscow: Metallurgiya, 1986.
18. Udovik, O.A., Yakobshe, R.Ya., and Efimov, V.A., Poisson's Ratio at the Solidification Temperature, *Progressivnye sposoby polucheniya stal'nykh slitkov* (Progressive Methods of Steel-Ingot Production), Kiev: Institute Problem Lit'ya, 1980, pp. 158–161.
19. Skok, Yu.Ya., Steel Failure Close to the Solidus Temperature, *Stal*, 1994, no. 3, pp. 27–30.
20. Nakagawa, T., Umeda, T., Murata, J., and Niwa, N., Deformation Behavior during Solidification of Steel, *ISIJ Intern.*, 1995, vol. 35, no. 6, pp. 723–729.

16 Studencheskaya St., Yekaterinburg, Russia, 620137 Tel: +7 (343) 374-03-80, fax: +7 (343) 374-29-23
E-mail: aup@vniimt.ru, website: www.vniimt.ru
A/c 40702810902400230701 in Yekaterinburg affiliate of NOMOS-BANK (JSC) Yekaterinburg
Correspondent account No.30101810800000000918, BIK 046577918, INN 6660011779, KPP 667001001, OKVED 73.10 OKPO 00190259

OJSC Scientific-Research Institute of Metallurgical Heat Engineering (VNIIMT) established in 1930 as Ural Division of All-Union Heat Engineering Institute is widely known in Russia and the CIS. The Institute focuses on development of high-technology heat engineering units, energy efficient and ecologically friendly technologies in ferrous and non-ferrous metallurgy, machine-building and other fuel-consuming branches of industry.

Highly-qualified academic researchers, unique experimental and production facilities and own research and design centre enable efficient scientific-and-research, design-and-experimental, engineering and project works, delivery of equipment, designer's supervision and commissioning works including execution of turnkey contracts in the following areas:

Sintering:

- development of techniques and modes of metal raw material heat treatment;
- design of energy-efficient agglomeration hearths and agglomeration gas heat recovery circuits allowing to reduce energy consumption and dust and gas emissions.

Pellet production:

- optimal traveling grate pelletizing furnaces for heat treatment of iron-ore pellets from various concentrates (hematite, magnetite, etc.) with optimal automatic process control system.

Preparation of metallic and nonmetallic raw materials:

- technique of iron-ore raw material dephosphorization by roasting and leaching;
- installations for drying high-moisture dispersive materials of various designs;
- efficient techniques of magnetizing roasting and subsequent dressing;
- technique of rare-earth element extraction (for example, germanium from germanium iron ores).

Blast-furnace ironmaking:

- explosion-proof near-furnace systems of blast furnace slag granulation giving a high-quality product for cement production;
- optimal control system for hot blast stoves;
- an innovative bench for drying hot metal and steel-smelting ladles;
- copper coolers and tuyeres of blast furnaces.

DRI (direct reduction of iron)

- improvement of the reduction technique in shaft furnaces for radical improvement of technical and economic indicators of their operation (productivity is increased twice);
- technique of raw material reduction in rotary furnaces using coal as the reductant.

Lime production: development of the technique and increase of lime production process efficiency:

- in shaft furnaces;
- in double-shaft furnaces;
- in rotary furnaces;
- in “stacked-tower preheater - rotary furnace” installations;
- in “shaft calciner - rotary furnace” installations (VNIIMT innovative technology).

Granulation of metal melts:

- development of technologies and designs of explosion-proof plants for near-furnace granulation of metallurgical slag, molten metal, etc., including heat recovery;

Reheating furnaces:

- development of new and update of the existing designs of furnaces for stock heating;
- high-performance systems of reheating furnace firing with recovery and regeneration firing systems based on the innovative burner units designed by VNIIMT;
- switching the furnace firing systems to cheaper fuel types;
- development and implementation of optimal furnace operating parameters.

Heat-treatment furnaces development of techniques and equipment for heat treatment of roll stock and metal products including those with protective atmospheres:

- thermochemical treatment conditions ensuring retention or directional change in chemical composition of metal surface;
- gas dampers for heat-treatment furnaces;
- spray quenching units and other elements of convective cooling systems;

Furnaces with protective atmosphere and gas treatment units:

- development of the furnace structure, design, manufacture, delivery and commissioning works;
- development of a technology for treatment of articles and devices for protective gas generation;
- calculation, development and manufacture of endogas and exogas atmosphere generators for metal product thermochemical treatment units;
- gas analysis systems for monitoring and control of physico-chemical properties of protective process atmospheres.

Reheating, heat-treatment and drying furnaces with convection heat transfer:

- development, design and manufacture using industrial heat-resistant (up to 900 ^{o}C) furnace fans designed by VNIIMT.

Rolled products:

- techniques and units for controlled high-speed air-to-water cooling (quenching) of rolled ferrous and non-ferrous metal products including thick plate on mill 5000;
- replacement of oil quenching technology with VNIIMT's eco-friendly air-to-water technique;
- innovative technique of oily mill scale processing;
- line of wire rod accelerated air cooling with process improvement.

Manufacturing manufacture and delivery of:

- high-performance burner units;
- heat-resistant (furnace) fans (up to 900 ^{o}C);
- copper coolers for blast furnaces and nonferrous furnaces based on VNIIMT technology;
- Pitot tubes for measuring flow rates and pressures.

OJSC VNIIMT developments are widely used in metallurgical enterprises of Russia, Ukraine, Kazakhstan, China, India and others.

For detailed information on institute developments, please visit OJSC VNIIMT site at www.vniimt.ru

Contact details:
Lik Zajnullin
General Director
OJSC VNIIMT
Tel: +7 (343) 374-03-80, fax: +7 (343) 374-29-23
16 Studencheskaya St., Yekaterinburg, Russia**,** 620137,
e-mail: aup@vniimt.ru,
website: www.vniimt.ru